Applications of ^{19}F NMR Spectroscopy To Studies On Intact Tissues

Alice M. Wyrwicz

Department of Radiology[1]
and MRI Center
University of Illinois at Chicago
Chicago, IL 60680

Contents

I. Introduction

In recent years the applications of NMR spectroscopy to the analysis of living systems have grown at a rapid pace. Initially these measurements were limited to excised tissues, and later extended to studies of perfused organs. With the new improvements in magnet technology and FT NMR techniques, *in vivo* measurements of intact animals and humans became possible. Most of these studies concentrated on the measurement of endogenous phosphorylated compounds with ^{31}P NMR spectroscopy which provided information on the bioenergetic and metabolic status of the tissues. Several excellent reviews on this topic are available (1,2). Other nuclei such as ^{13}C, ^{23}Na, ^{1}H, and ^{19}F have also been used as probes of metabolic changes taking place in tissues under varied physiological and pathological conditions.

In vivo ^{19}F NMR spectroscopy is a relatively new technique, with the first ^{19}F surface coil study of an intact animal reported in 1983 (3). This nuclide is well suited to study the metabolic fate of exogenously administered substances such as flourinated drugs, many of which are in clinical use. Fluorine-19 is the 100% abundant isotope of elemental fluorine, has a spin 1/2, NMR sensitivity about 83% that of proton and it occurs in living systems in trace amounts. The large chemical shift range of ^{19}F (over 900 ppm) permits spectroscopic differentiation of similar compounds even at the lower field strengths used in the *in vivo* experiments. These characteristics make ^{19}F an excellent NMR probe with which to monitor the distribution, retention or metabolism of drugs (or other compounds) in specific organ systems. Thus, it provides a potentially powerful method to evaluate the biochemical mechanisms involved in these processes.

This article discusses applications of *in vivo* ^{19}F NMR spectroscopy to the metabolic studies of three distinct classes of fluorinated compounds of biological importance. These are: fluorodeoxyglucose an-

[1]Present Address: Department of Medicine, Evanston Hospital, Evanston, IL 60201

alogs, fluorinated antitumor agents, and fluorinated general anesthetics.

II. Fluorodeoxyglucose Analogs

The basic substrate for brain metabolism, under normal conditions, is glucose. To measure the local rates of glucose utilization, methods were developed based upon the use of the radioactively labelled analogs of glucose, [^{14}C] 2-deoxy-D-glucose or [^{18}F] 2-fluoro-2-deoxy-D-glucose, rather than glucose itself (4,5). These analogs were selected because of their biochemical properties. They are transported by the same carrier as glucose and are phosphorylated to their corresponding 6-phosphates by the hexokinase in the brain tissue (6,7). Unlike the glucose 6-phosphate, which is further metabolized, 2-DG-6-P or 2-FDG-6-P are considered trapped in the brain tissue since they cannot be converted to fructose-6-phosphate and are not considered to be substrates for glucose-6-P dehydrogenase (8). Thus, these analogs have been said to isolate the first step in the biochemical pathway of glucose metabolism, the hexokinase catalyzed phosphorylation of the hexose.

Although glucose analogs have been extensively used in studies of regional metabolism in the brain, controversy still exists as to the level of phosphatase activity in the brain (9-12) and the extent of dephosphorylation of the 6-phosphates by this enzyme during the time interval of the autoradiographic or PET studies. Since these techniques are based on measurement of product accumulation, it is essential that the product i.e. DG-6-P or FDG-6-P (and their derivatives) be trapped in the brain tissues, at least for the duration of the measurement.

Individual metabolic products containing these radioactive labels cannot be distinguished by these techniques, which rely on the measurement of total radioactivity. However, *in vivo* ^{19}F NMR studies of 2-FDG have shown considerable metabolism extending beyond the FDG-6-phosphate stage (13-17). Unlike the ^{31}P NMR measurements which monitor only the initial phosphate-containing products (18), the ^{19}F NMR spectroscopy detects all the fluorinated products formed. A typical *in vivo* NMR spectrum of rat brain 2 h after 2-FDG administration (Figure 1) shows five peaks with distinct ^{19}F chemical shifts (15). However, the large linewidths associated with these peaks limit the spectral resolution and the information which can be extracted from it. Thus under these experimental conditions one cannot resolve the ^{19}F signals from free and phosphorylated 2-FDG because of the small differences between their chemical shifts which is within the line width of the observed peak. Presence of both α and β anomers of the two compounds further increases the number of overlapping signals. For comparison a corresponding spectrum of brain tissue extract is shown in Figure 2. Four of the five signals observed *in vivo* are visible in much greater detail here. The higher magnetic field (9.4 T) used in these extract studies affords better chemical shift dispersion and permits good resolution of all the multiplets. The extract spectrum shows the presence of both α and β anomers of 2-FDG, 2-FDG-6-phosphate, 2-FDM and 2-FDM-6-phosphate (19). Earlier reports suggested that pentose monophosphate shunt (PMS) and aldose reductase sorbitol (ARS) pathways are involved in the elimination of this compound from the brain (20,21). There is no evidence that products of the ARS pathway are present in the brain tissue extracts (19,22). The PMS pathway is of importance only at high 2-FDG doses; at lower doses the (phospho)gluconate peak is not observed in the extracts although it is clearly seen in the *in vivo* spectra. The Harderian/lacrimal glands which contain very high levels of this compound (19,22), may contribute to this signal observed in the *in vivo* ^{19}F NMR spectra of the "brain". The active volume of the surface coil used in the *in vivo* measurements could include these glands. To avoid any contribution from other tissues in close proximity to the brain, a localized NMR technique on anatomically defined areas of interest needs to be employed.

The temporal profiles generated by the surface coil ^{19}F NMR studies of cerebral 2-FDG metabolism are shown in Figure 3. Normalized peak areas (proportional to concentration) of the individual resonances, as well as the total fluorine-19 signal observed in the rat brains after 2-FDG infusion, were used to generate these profiles. Curve A, which represents the total ^{19}F signal area, passes through a maximum at 15-20 min after 2-FDG infusion and then decays with a half-life of 210 $\pm$ 10 min. Curve B illustrates changes with time in the area of the ^{19}F signal at -123.4 ppm (peak b in Figure 1). This signal corresponds almost entirely to 2-FDG-6-P.

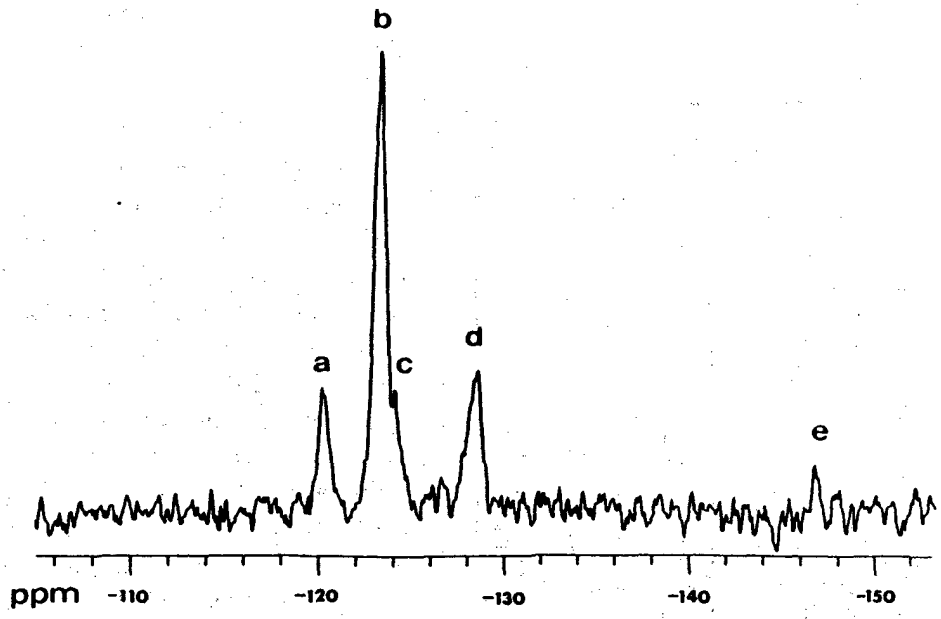

Figure 1: Surface-coil ^{19}F NMR spectrum from intact rat brain 2 hours after a bolus injection of 50 mg 2-FDG; (a) 2-fluoro-2-deoxy-6-phosphogluconate, (b) 2-fluoro-2-deoxy-D-glucose and 2-fluoro-2-deoxy-D-glucose-6-phosphate (α and β anomers), (c) unassigned, (d) α-2-fluoro-2-deoxy-D-mannose and α-2-fluoro-2-deoxy-D-mannose-6-phosphate, (e) β-2-fluoro-2-deoxy-D-mannose and β-2-fluoro-2-deoxy-D-mannose-6-phosphate. Acquisition parameters: pulse width, 14 μsec at 100 W; spectral width, 20KHz; 8 k data points; pulse repetition rate 1.8 s; accumulation time 30 min (three 10 min block averages). Chemical shifts are reported relative to an external 10mM TFA (from reference 15).

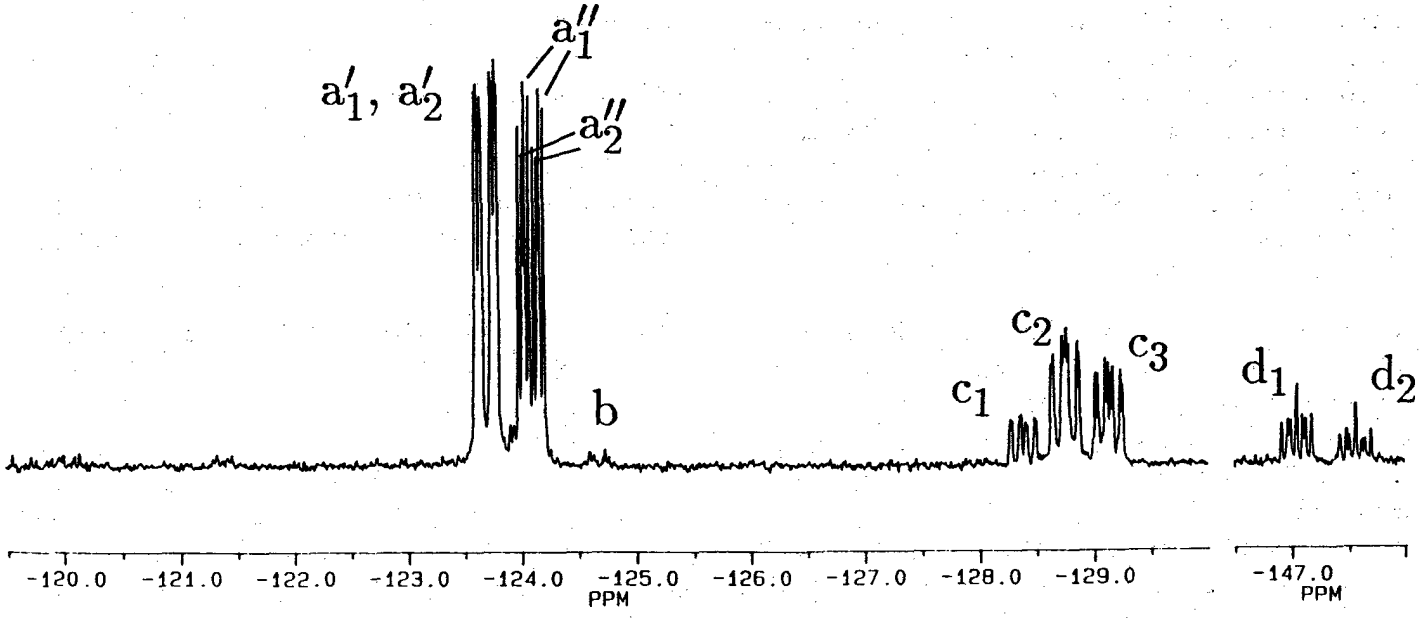

Figure 2: ^{19}F NMR spectra of the brain extracts obtained 2 hours after a bolus injection of 50 mg of 2-FDG in 1 ml saline. (a'_1) β-2-FDG-6-phosphate; (a''_1) α-2-FDG-6-phosphate; (a'_2) β-2-FDG; (a''_2)α-2-FDG; (b) and (c_1) unassigned; (c_2) α-2-FDM; (c_3) α-2-FDM-6-phosphate; (d_1) β-2-FDM-6-phosphate; (d_2) β-2-FDM. The chemical shifts are referenced to external 10 mM TFA.

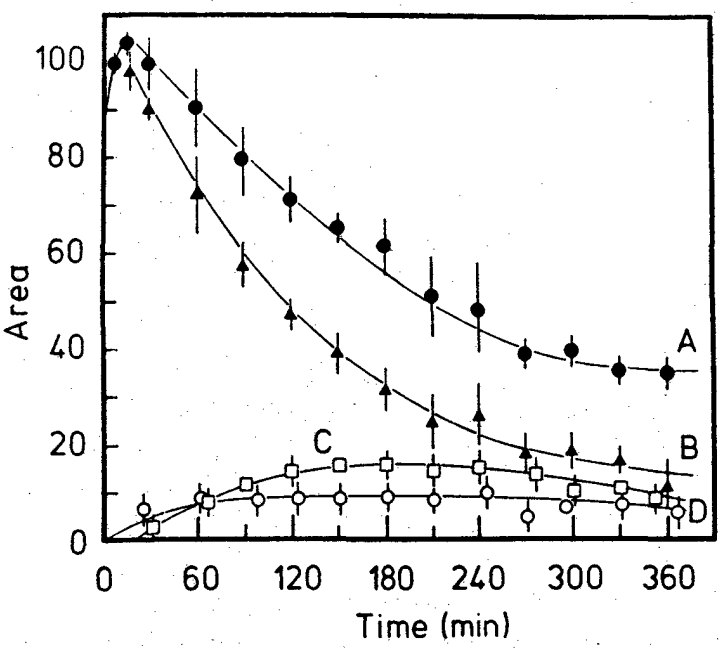

Figure 3: Uptake and elimination of 2-FDG in rat brain after a bolus iv infusion of 50 mg in 1 ml saline. The data plotted in this figure represents the results of the integration of the total and individual ^{19}F resonances observed following 2-FDG infusion. Spectra resulting from data acquisition over the first 30 min after injection were integrated and assigned an arbitrary value of 100 for total ^{19}F signal. All other signal areas have been assigned relative to this value. Curve A represents the total ^{19}F signal area; curve B, ^{19}F signal area at -123.4 ppm; curve C, ^{19}F signal area at -120.4 ppm, curve D, ^{19}F signal area from -126.0 to -130.4 ppm. The results presented are for five animals.

The estimated half-life for this metabolite in brain is 105 ± 5 min, reasonably close to the 80 min reported for a lower dose of 2-FDG (17). The low dose experiments show a well-defined plateau occurring from 10-70 min after injection, not observed in the higher doses studies. These half-lives are different from the 8 h estimated for 2FDG using [^{18}F] 2-FDG (5) but not significantly different from the half-life for [^{14}C] 2-DG (23). The NMR experiments provide biochemical information on the cerebral metabolism of 2-FDG not available from the PET or autoradiographic studies. However, much higher doses of this compound required for the NMR studies generated concern over their relevance. Dose dependent effects are reflected in the relative abundances of phosphorylated and non-phosphorylated species observed, with non-phosphorylated metabolic products present at higher doses used (22). The pentose monophosphate shunt is of importance only at high 2-FDG levels (16,22). The major metabolic products, 2-FDG-6-P and the 2-FDM-6-P, remain the same. The interconversion of 2-FDG-6-P to 2-FDM-6P is catalyzed in the brain by phosphoglucose isomerase (22,24).

Another glucose analog, 3-fluoro-3-deoxy-D-glucose (3-FDG), was used as a probe of the aldose reductase activity in the brain (25). The 3-FDG is transported by the same carrier as glucose, but unlike 2-FDG, it is not phosphorylated in the brain tissue by hexokinase (7). It is also not considered to be a substrate for glucose-6-P dehydrogenase (8). Instead it is metabolized in the brain exclusively to 3-fluoro-3-deoxy-D-sorbitol (3-FDSL) and 3-fluoro-3-deoxy-D-fructose (3-FDF) via the aldose reductase sorbitol pathway (Figure 4). Pretreatment of the animal with an aldose reductase inhibitor, sorbinil, inhibits the formation of sorbitol (25). The ARS pathway is a major pathway for glucose metabolism in several different organs, including the brain; it bypasses the control points of hexokinase and phosphofructokinase (26) and provides a competitve energy source.

3-FDG has the potential to noninvasively monitor the aldose reductase activity in tissues under normal and pathological conditions, and to test the effectiveness of different inhibitors of this enzyme. This compound can be used in high doses required by the NMR studies because of its low toxicity (27).

III. Fluorinated Antitumor Agents

Nucleoside analogs such as the fluorinated pyrimidines, 5-fluorouracil (5-FU), 5-fluorouridine (5-Urd) and 5-fluoro-2-deoxyuridine (FdU), are widely used as chemotherapeutic agents in the treatment of human cancers (28,29). Two major effects are observed in cells upon treatment with these compounds: (1) inhibition of DNA synthesis by inhibition of dTMP synthetase by fluorodeoxyuridine monophosphate (FdUMP) (30); and (2) extensive incorporation of 5FU in place of uracil resulting in changes in the processing and function of some types of RNA (30,31). It is not clear which of these effects

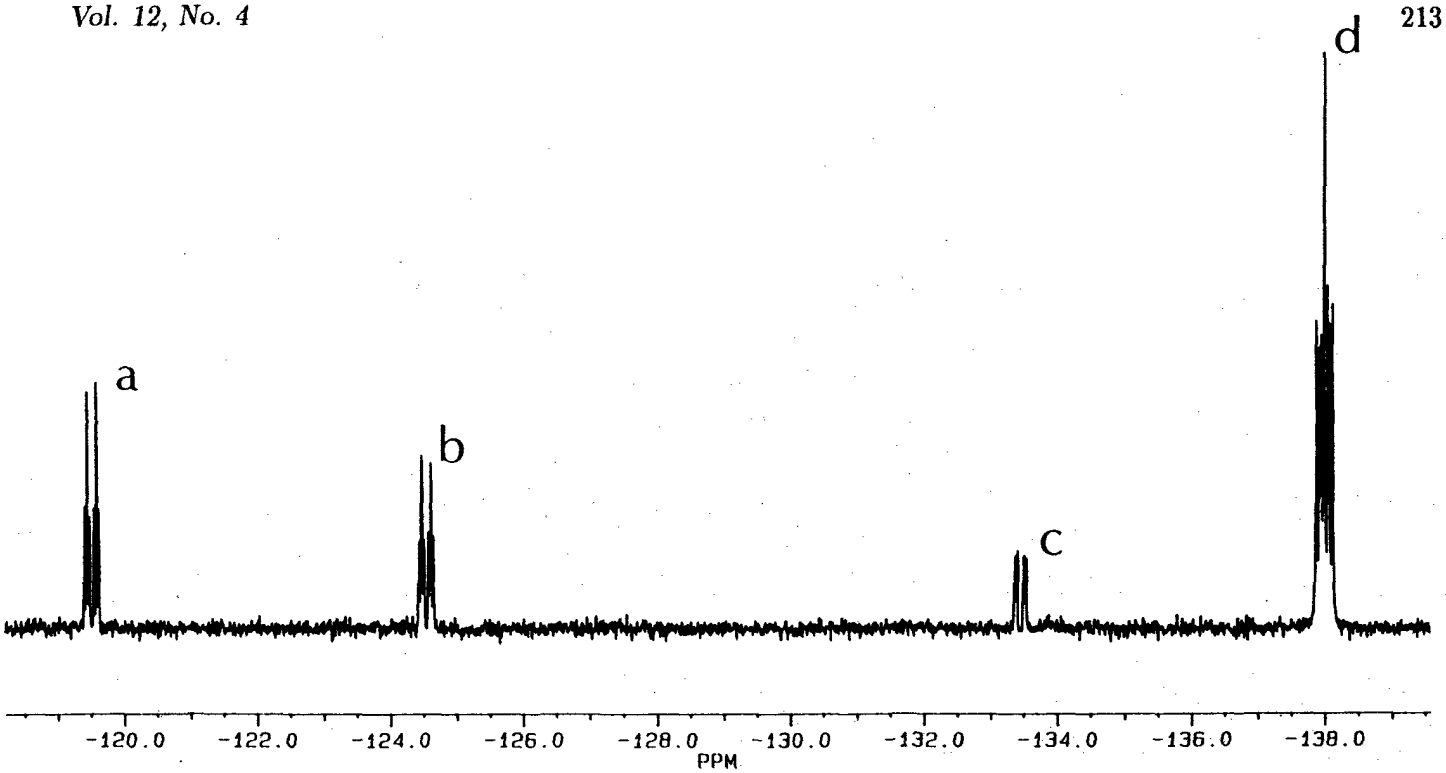

Figure 4: ^{19}F NMR spectrum of brain extract obtained 2 hrs after a bolus injection of 50 mg of 3-FDG. (a) α-3-FDG; (b) β-3-FDG; (c) 3-fluoro-3-deoxy-D-fructose; (d) 3-fluoro-3-D-sorbitol. Chemical shifts are relative to external 10 mM TFA.

accounts for the major antitumor property of these drugs. The therapeutic efficacy of these compounds, as of any other drug, depends on their uptake and the rate of their metabolism at the site of action and the site(s) of detoxification. This information can be provided directly and noninvasively with *in vivo* ^{19}F NMR spectroscopy.

The first *in vivo* ^{19}F studies of 5-FU were carried out in implanted Lewis lung carcinomas and livers of C57 mice using surface coils (32). Two fluorinated metabolites identified as dihydrofluorouracil (FUH) and α-fluoro-β-alanine (FABL), the end product of 5-FU metabolism, were observed in the liver. Similar ^{19}F NMR spectra were observed for rabbit liver after the treatment with 5-UF (33). The peak tentatively identified as FUH was later shown to correspond to fluoro-β-ureidopriopionic acid (FUPA) (33,34). Spectra of the implanted tumors showed no catabolic products detected in the liver, only the active compound, fluorodeoxyuridine monophosphate (FdUMP). Since the formation of this compound was barely detectable at the lower doses used, it was suggested that most of the FdUMP was in an environment invisible to NMR, possibly bound to a protein. Simultaneous administration of thymidine with 5FU resulted in formation of a toxic deoxyuracil derivative, fluorouracil deoxyribose (5FUdR) in liver. This is consistent with the finding that thymidine induces synthesis of thymidine phosphorylase which catalyzes the conversion of 5FU to the toxic 5FUdR (35). As expected, conversion of 5FU to fluoronucleotides in tumor cells is inhibited by allopurinol (36).

The *in vivo* ^{19}F NMR metabolic studies of 5FU were extended to cancer patients undergoing chemotherapy with 5-FU, each receiving a therapeutic dose of approximately 20 mg/kg (37). ^{19}F NMR spectra acquired with a surface coil placed over the liver of a patient are shown in Figure 5. Only the end metabolic product, FBAL, is observed over the course of 3 hours. No intermediary metabolic products such as FUPA, observed before in rodents, are visible in these spectra. The inability to observe FUPA is most likely due to a nine-fold lower dose used in the human studies. The half-life of unmetabolized 5-FU in the liver was estimated to be approximately 20 min. Unmetabolized 5-FU was also observed in the tumors of patients with breast and colon carcinoma undergoing 5-FU chemotherapy (38). No other metabolic products were detectable in the ^{19}F NMR spectra of the tumors. The half-life of 5-FU in these tumors varied from 0.4 to

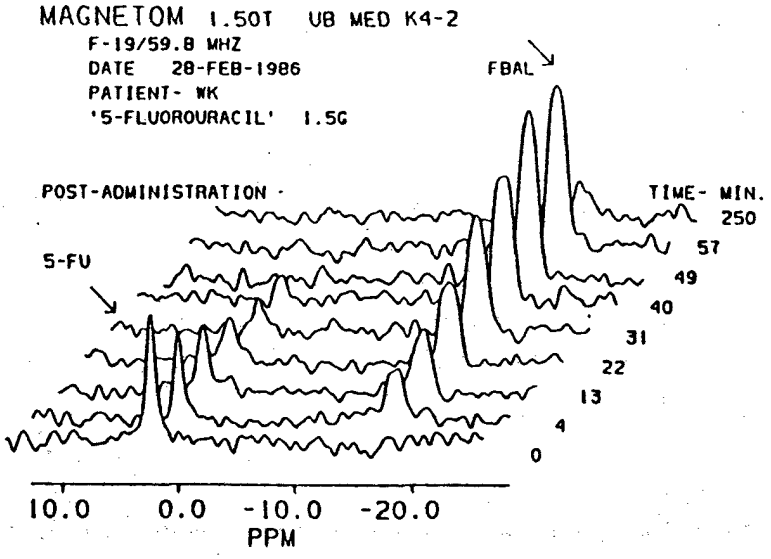

Figure 5: Serial ^{19}F spectra acquired with a surface coil over the liver of a patient in a 1.5 T MRI system, operating at 59.8 MHz for ^{19}F. Each spectrum is the result of 128 FIDs using a 250 μs 90 pulse with 512 complex points collected over a period of 8.5 min (from reference 37).

2.1 hours, much longer than any other tissue studied. This accumulation or "trapping" of free 5-FU was suggested to provide means for assessing the effectiveness of 5-FU therapy. A more recent study of 11 patients confirmed that a patient's response to chemotherapy correlates with the extent of trapping of free 5-FU in the human tumors (39).

These results demonstrate that in addition to basic studies on drug metabolism, ^{19}F NMR spectroscopy can be applied to cancer patient management by optimizing and individualizing the patient's drug regimens. A more detailed review on fluorinated pyrimidines appeared recently (40).

IV. Fluorinated Anesthetics

Fluorinated hydrocarbons and ethers such as halothane ($CF_3CHClBr$), isoflurane (CF_3CHCl-O-CF_2H) and enflurane ($CHClF$-CF_2-O-CF_2H) are the most often used general inhalation anesthetics. Once taken up by the lungs, they enter the circulatory phase during which transfer from arterial blood to brain and other organs occurs. Their concentrations in tissues are in the millimolar range and depend on the dose administered and the duration of delivery.

The first *in vivo* surface coil study demonstrated that fluorinated anesthetics could be observed in brain tissue and that anesthetic clearance could be monitored (3). The results of these measurements were unexpected and contrary to the belief that volatile anesthetic agents are quickly eliminated after their administration is discontinued. Instead, they showed that halothane clearance from the brain was relatively slow as compared to the recovery from anesthesia, and that a halothane metabolite or adduct remained in the brain at measurable levels for several days. Subsequent, more detailed studies confirmed the initial findings and identified the long-lived fluorine-containing species as trifluoroacetate, a known metabolite of halothane (41). The same studies showed that halothane exists in two different environments in the brain, characterized by different half-lives and different ^{19}F chemical shifts (Figure 6). The environment with the short half-life (25 min) corresponds closely to the clinical recovery from halothane and thus may represent sites involved in the anesthesia phenomenon. The *in vivo* results were corroborated by *ex vivo* experiments on the excised brain tissue.

Halothane elimination from rat brain (42) was also characterized by two component decay and the short half-life (34 min) was close in value to the one reported for the rabbits (25 min). The second, longer component of the elimination curve was not clearly defined, however, these two studies differed considerably in the experimental design. No ^{19}F resonance for halothane metabolite was reported in rat

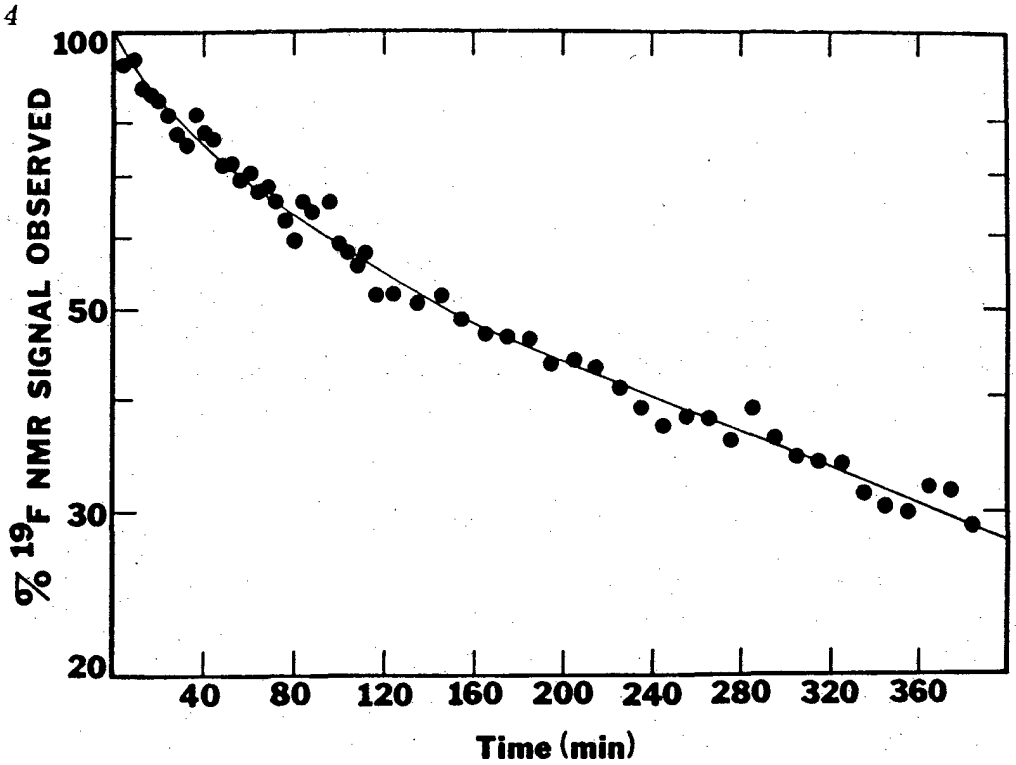

Figure 6: A representative time course of halothane elimination from rabbit brain after 90 min exposure to 1% halothane. Fluorine-19 signal areas are expressed as percent signal remaining in the brain plotted against time (from reference 38).

brain, probably due to the large linewidths seen in those spectra (42). No extracts of brain tissue were studied, which would have demonstrated whether significant concentrations of halothane metabolites were present. Recent rotating frame zeugmatography experiments of halothane distribution in a rat head (43) clearly show the presence of halothane metabolite observed before in a rabbit brain. The spatial and temporal distribution of the metabolite is quite different from that of the parent compound, halothane.

Two environments of halothane in excised brain, as characterized by T_2 relaxation times, were observed recently (44). The environment characterized by a T_2 of 3.6 ms was shown to be saturable at halothane levels in brain that produce clinical anesthesia. The second environment, characterized by a T_2 of 43 ms was not saturable at physiological concentrations. This long T_2 environment, which only becomes evident after extended halothane exposure at high concentrations, resembles halothane in synthetic liposomes (45). It is present exclusively in the white matter of the brain whereas the short T_2 environment is present in both gray and white matter (46). The environment(s) characterized by the short T_2 is consistent with anesthetic action indicating that a single saturable halothane site in the brain is responsible for anesthesia. Later reports attributed this finding to anesthetic-induced depression of halothane uptake into the blood (47,48). However these reports do not unequivically exclude saturable binding sites for anesthetics in the brain.

Studies of the elimination of isoflurane from rabbit brain have also been reported (Figure 7). Like halothane, isoflurane elimination can be characterized as a two-component decay with half-lives of 26 and 174 minutes (49). The shorter half-life is equal to that observed for halothane (25 min), whereas the longer half-life is significantly less than that for halothane. This data again suggests that the cellular environment characterized by the shorter half-life includes the anesthetic molecules responsible for anesthesia. Another study reported somewhat longer half-life (36 min) for the fast decaying component of the isoflurane elimination (50).

The use of halothane as a surgical anesthetic occasionally results in severe liver damage, termed halothane hepatitis (51). Halothane hepatitis may be caused by the formation of a harmful halothane metabolite in liver (52). Preliminary studies of halothane metabolism in rat (53) and rabbit liver (54) indicate that hepatic halothane metabolism

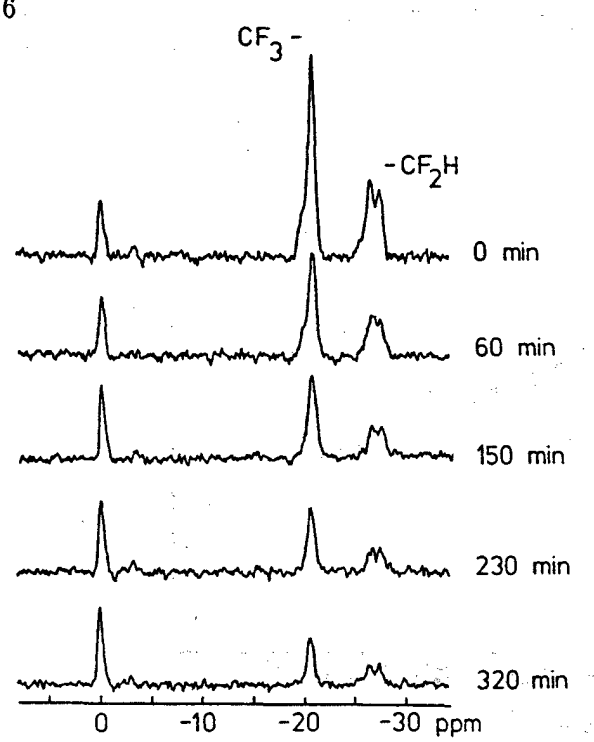

Figure 7: *In vivo* surface coil ^{19}F NMR spectra of rabbit brain at various times (90-320) min following isoflurane anesthesia. Chemical shifts are reported relative to the resonance of an external standard of 2.5% $C_2Br_2F_4$ in $CHCl_3$ which was set at ppm.

could be successfully monitored. An *in vivo* study examining halothane metabolism in the liver of intact rats showed only one metabolite, trifluoroacetic acid, visible under normal anesthesia conditions (55). Studies of anaerobic halothane metabolism in rat liver homogenates demonstrated that ^{19}F NMR spectroscopy can be used to monitor the complete metabolism of halothane to trifluoroacetic acid, chlorotrifluoroethane, chlorodifluoroethane, and inorganic fluoride (56).

^{19}F NMR has also been used to answer questions about the hepatic metabolism of methoxyflurane (57), the dose dependent elimination of methoxyflurane from rat liver has been reported. Also, possible mechanisms of hepatic methoxyflurane metabolism have been evaluated in these studies.

V. References

[1]D. P. Holis, "Biological Magnetic Resonance" **2**, 1-44, Plenum Press, New York.

[2]G. A. Elgavish, "Biological Magnetic Resonance", **2**, 1-81, Plenum Press, New York.

[3]A. M. Wyrwicz, M. H. Pszenny, J. C. Schofield, P. C. Tillman, R. E.Gordon and P. A. Martin, *Science* **222**, 428 (1983).

[4]L. Sokoloff, M. Reivich, C. Kennedy, M. H. Des Rosiers, C. S. Patlak, K. D. Pettigrew, O. Sakurada and M. Shinohara, *Neurochem.* **28**, 897 (1977).

[5]M. Reivich, D. Kuhl, A. P. Wolff, J. Greenberg, M. Phelps, T. Ido, V. Cassella, J. Fowler, E. Hoffman, A. Alavi, P. Som, L. Sokoloff, *Circ. Res.* **44**, 127 (1979).

[6]A. Sols and R. K. Crane, *J. Biol. Chem.* **210**. 581 (1954).

[7]E. M. Bessel, A. B. Foster, J. H. Westwood, *Biochem. J.* **128**, 199 (1972).

[8]E. M. Bessel and P. Thomas, *Biochem. J.* **131**, 83 (1973).

[9]T. Nelson, S. Lucignani, S. Atlas, A. M. Crane, G. A. Daniel and L. Sokoloff, *Science* **229**, 60 (1985).

[10]W. Sacks, S. Sacks and A. Fleischer, *Neurochem. Res.* **8**, 661 (1983).

[11]M. T. Huang and R. L. Veech, *J. Biol. Chem.* **257**, 11358 (1982).

[12]T. Nelson, G. Lucignani, J. Goochee, A. M. Crane and L. Sokoloff, *J. Neurochem.* **46**, 905 (1986).

[13]T. Nakada, I. L. Kwee, C. B. Conboy, *J. Neurochem.* **46**, 198 (1986).

[14]B. A. Berkowitz and J. J. H. Ackerman, *Soc. Magn. Reson. Med.* **4**, 759 (1985) Abst.

[15]A. M. Wyrwicz, R. Murphy, J. Prakash, R. Moriarty and T. Dougherty, *Soc. Magn. Reson. Med.* **4**, 827 (1985) Abst.

[16]N. R. Bolo, K. M. Brennan, R. M. Jones and T. F. Budinger, *Ann. N.Y. Acad. Sci.* **508**, 451 (1987).

[17]B. A. Berkowitz, S. K. Songs, R. K. Deuel, J. J. H. Ackerman, *Soc. Magn. Reson. Med.* **7**, 109 (1988). Abst.

[18]R. K. Deuel, G. M. Yue, W.R.Sherman, D. J. Schickner, J. J. H. Ackerman, *Science* **228**, 1329 (1985).

[19]R. Pouremad and A. M. Wyrwicz, *Soc. Magn. Reson. Med.* **7**, 93 (1988). Abst.

[20]Nakada, I. L. Kwee, *Biochem Arch.* **2**, 53 (1986).

[21]T. Nakada and I. L. Kwee, *Magn. Reson. Med.* **4**, 366 (1987).

[22]R. Pouremad and A. M. Wyrwicz, *NMR in Biomedicine*, in press.

[23]R. A. Hawkins and A. L. Miller, *Neurosci.* **3**, 251 (1978).

[24]Y. Kanazawa, Y. Momozono, H. Yamane, T. Hardahira, M. Maeda, and M. Kojima, *Chem. Pharm. Bull.* **35**, 895 (1987).

[25]I. L. Kwee, T. Nakada and P. J. Card, *J. Neurochem.* **49**, 428 (1987).

[26]J. Jeffery and H. Jornvall, *Proc. Natl. Acad. Sci. USA* **80**, 901 (1982).

[27]J. R. Halama, S. J. Gatley, T. R. DeGrado, D. R. Bernstein, C. K. Ng, and J. E.Holden, *Am. J. Physiol.* **247**, H734 (1984).

[28]K. L. Mukherjee, J. Boohar, D. Wentland, F. J. Ansfield, C. Heidelberger, *Cancer Res.* **23**, 49 (1963).

[29]B. A. Chabner in "Cancer and Chemotherapy," (S. T. Crook, Ed.), Academic Press, New York (1981).

[30]C. Heidelberg, in "Antineoplastic and Immunosuppresive Agents," Vol. 38, p.193, (A. C. Sartorelli and D. G. Johns, Eds.) Springer Verlag, New York (1974).

[31]C. K. Carrico and R. I. Glazer, *Cancer Res.* **39**, 3694 (1979).

[32]A. N. Stevens, P. G. Morris, R. A. Iles, P. W. Sheldon and J. R. Griffiths, *Br. J. Cancer* **50**, 113 (1984).

[33]J. Bernadou, J. P. Armand, A. Lopez, M. C. Malet-Martino, *Clin. Chem.* **31**, 846 (1985).

[34]M. C. Malet-Martino, R. Martino, A. Lopez, J. P. Beteille, M. Bon, J. Bernadou, and J. P. Armand, *Biochem. Pharmacol.* **34**, 429 (1985).

[35]B. Ardalan and R. Glazer, *Cancer Treat. Rev.* **8**, 157 (1981).

[36]M. J. W. Prior, P. M. J. McSheehy, R. J. Maxwell, and J. R. Grffiths, *Soc. Magn. Reson. Med.* **6**, 502 (1987).

[37]W. Wolf, M. J. Albright, M. S. Silver, H. Weber, U. Reichardt and R. Sauer, *Mag. Reson. Imag.* **5**, 165 (1987).

[38]W. Wolf, C. A. Presant, K. L. Servis, A. El-Tahtawy, M. J. Albright, P. B. Barker, R. Ring III, D. Atkinson, R. Ong, M. King, M. Singh, M. Ray, C. Wiseman, D. Blayney, and J. Shani, *Proc. Natl. Acad. Sci.* **87**, 492 (1990).

[39]C. A. Presant, W. Wolf, M. J. Albright, K. L. Servis, R. Ring III, D. Atkinson, R. L. Ong, C. Wiseman, M. King, D. Blayney, P. Kennedy, A. El-Tahtawy, M. Sing, and J. Shani, *J. Clin. Oncol.* **8**, 1868 (1990).

[40]P. M. J. McSheehy and J. R. Griffiths, *NMR in Biomedicine* **2**, 133 (1989).

[41]A. M. Wyrwicz, C. B. Conboy, B. G. Nichols, K. R. Ryback, and P. Eisele, *Biochim. Biophys. Acta* **929**, 271 (1987).

[42]L. Litt, R. Gonzalez-Mendez, T. L. James, D. I. Sessler, P. Mills, W. Chew, M. Moseley, B. Pereira, J. W. Severinghaus, W. K. Hamilton, *Anesthesiology* **67**, 161 (1987).

[43]C. B. Conboy and A. M. Wyrwicz, *Magn. Reson. Med.* **9**, 219 (1989).

[44]A. S. Evers, B. A. Berkowitz and D. A. d'Avignon, *Nature* **328**, 157 (1988).

[45]L. S. Kohler, E. T. Fossel, and K. A. Kohler, *Biochemistry* **16**, 3700 (1977).

[46]M. Miyazaki, E. Shen and A.M. Wyrwicz, *Biophys. J.* **57**, 44a (1990).

[47]A. S. Evers, B. A. Berkowitz and D. A. d'Avignon, *Nature* **341**, 766 (1989).

[48]S. H. Lockhart, Y. Cohen, N. Yasuda, F. Kim, L. Litt, E. I. Eger II, L. -H. Chang, T. L. James, *Anesthesiology* **73**, 455 (1990).

[49]A. M. Wyrwicz, C. B. Conboy, K. R. Ryback, B. G. Nichols, and P. Eisele, *Biochim. Biophys. Acta* **927**, 86 (1987).

[50]P. Mills, D. I. Sessler, M. Moseley, W. Chew, B. Pereira, T. L. James, and L. Litt, *Anesthesiology* **67**, 169 (1987).

[51]J. G. L. Stock and L. Strunin, *Anesthesiology* **63**, 424 (1985).

[52]J. L. Plumer, M. J. Cousins, and P. Hall, *Quart. Rev. Drug Met. Interact.* **4**, 49 (1982).

[53]C. T. Burt, R. R. Moore, M. F. Roberts, and T. J. Brady, *Biochim. Biophys. Acta* **805**, 375 (1984).

[54]F. F. Brown, M. J. Halsey, B. Wardlley-Smith, and P. A. Martin, *Proc. Anaesth. Res. Soc.* **806P** (1984).

[55]B. S. Selinsky, M. Thompson, L. M. Jeffreys, and R. E. London, *Biochem. Pharmacol.* **36**, 413 (1987).

[56]B. S. Selinsky, M. Thompson, L. M. Jeffreys, and R. E. London, *Biophys. J.* **49**, 329a (1986).

[57]B. S. Selinsky, M. E. Perlman, and R. E. London, *Mol. Pharmacol.* **B33**, 559 (1988).